

Variability of Middle Triassic vermicular limestone ichnofabrics: the Anisian Hisban Formation in Jordan

MICHAŁ STACHACZ¹, ALFRED UCHMAN¹, PIOTR JAGLARZ¹, ABDALLA ABU HAMAD²,
IKHLAS AL-HEJOJ² and HABES AL-MASHAKBEH³

¹ Institute of Geological Sciences, Jagiellonian University, Gronostajowa 3a, 30-387 Kraków, Poland;
e-mails: michal.stachacz@uj.edu.pl, alfred.uchman@uj.edu.pl, piotr.jaglarz@uj.edu.pl

² Environmental and Applied Geology Department, The University of Jordan, 11942 Amman, Jordan;
e-mail: a.abuhamad@ju.edu.jo

³ Applied Earth and Environmental Sciences Department, Faculty of Earth and Environmental Sciences,
Al al-Bayt University, P.O.BOX 130040, 25113 Mafraq, Jordan; e-mail: Habes2819@aabu.edu.jo

ABSTRACT:

Stachacz, M., Uchman, A., Jaglarz, P., Abu Hamad, A., Al-Hejoj, I. and Al-Mashakbeh, H. 2024. Variability of Middle Triassic vermicular limestone ichnofabrics: the Anisian Hisban Formation in Jordan. *Acta Geologica Polonica*, **74** (3), e22.

The strongly bioturbated Middle Triassic (Anisian) limestones, referred to as vermicular limestone, are the dominant lithology of the Hisban Formation in Jordan. This limestone exhibits the monotonous *Oravaichnium*–*Planolites* ichnofabrics, which are known and common in the northern Peri-Tethys and the Germanic Basin. The most abundant and widespread trace fossil here is *Oravaichnium carinatum*, which is produced by bivalves. Specimens of *O. carinatum* from the Hisban Formation are typically strongly elongated in the vertical axis and have a smooth surface, whereas specimens from the Germanic Basin mainly have a pear-shaped cross-section. Nevertheless, both morphologies and transitional morphotypes between these ichnospecies are present in both areas. The difficulty in distinguishing between *Oravaichnium* and *Planolites* causes the intense bioturbation by bivalves to be underestimated. The wide occurrence of the *Oravaichnium* ichnofabric in the northern and southern Peri-Tethys suggests that small burrowing bivalves played a significant role in the colonization and infaunalization during the long-term recovery of the benthos after the Permian–Triassic crisis. They experienced intense development during the Middle Triassic, when they were responsible for extensive bioturbation.

Key words: Trace fossils; Bivalve burrows; Bioturbation; Colonization; Tethys; Permian–Triassic recovery; Jordan.

INTRODUCTION

The vermicular limestones are a characteristic facies of the Tethyan and Peri-Tethyan Middle Triassic carbonate platforms, especially in the Anisian. They are distinguished by their typical monotonous ichnofabrics dominated by simple burrows, which are readily visible in the field. The relatively low diversity of trace fossils contributing to the ichnofabrics is related to severe environmental conditions,

mainly hypersalinity and low oxygenation (Jaglarz and Uchman 2010). Nevertheless, it appears that the composition of the ichnofabric is not uniform and varies from region to region. In some areas, simple burrows dominated by *Planolites* and referred to as “worms” prevail, e.g., in the Tatra Mountains in Poland (Jaglarz and Uchman 2010) or the Catalan Basin (Mercedes-Martín and Buatois 2021), but in other areas, *Balanoglossites* (produced probably by enteropneusts or annelids) or *Protovirgularia* (pro-



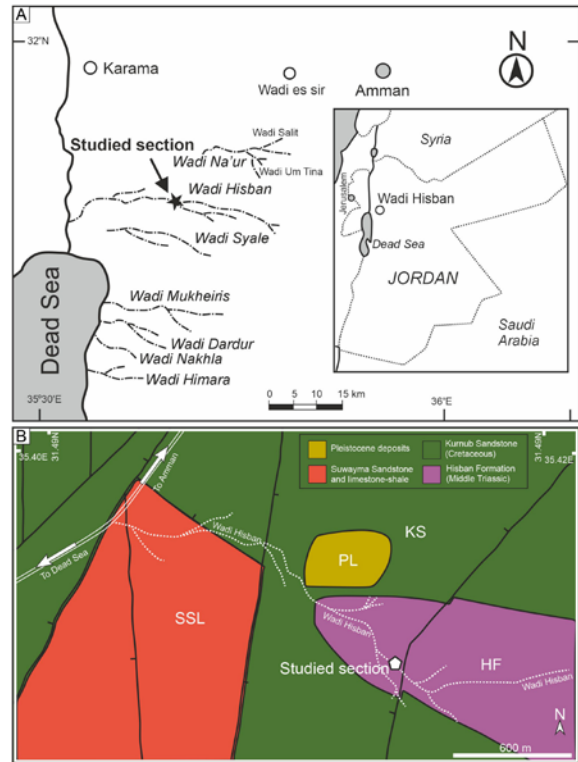
duced by bivalves or arthropods) are the dominant ichnotaxa, e.g., in Sardinia in Italy (Knaust and Costamagna 2010). This suggests that it is possible to separate different types of vermicular limestones on the basis of their ichnofabrics. At present, this can be demonstrated only for some places/areas, because most occurrences of vermicular limestones require new investigation, which includes analysis of their ichnofabrics.

In this paper, the vermicular limestones of the southern Peri-Tethys, Hisban Formation in Jordan are presented. They show an ichnofabric dominated by *Oravaichnium*, which is produced by bivalves. Such an ichnofabric has not previously been described, but interestingly, it is also present in the northern Peri-Tethys in some parts of the Muschelkalk Basin in Poland, Germany, and France.

GEOLOGICAL SETTING

Triassic of Jordan

The Permian–Triassic strata of Jordan are about 1000 m thick, of which about 600 m are exposed between Wadi Mujib in the south and Wadi Zarqa in the north. The nine formations distinguished by Bandel and Khoury (1981) are well recognizable in the field by their top and basal surfaces, with only the top of the Um Tina and Mukheiris formations and the base of the Abu Ruweis Formation not exposed. A three-part Triassic, as known from the classic German Basin, with Buntsandstein, Muschelkalk, and Keuper, is also found in Jordan, although details are different. The lower portions with the Ma'in, Dardur and the Ain Musa formations could be considered equivalent to the Buntsandstein, with a predominance of reddish quartz sandstone. The Hisban, Mukheiris and Iraq Al-Amir formations are predominantly marine, as is the Muschelkalk, and yield mainly limestones, even though near-terrestrial conditions occur, including plant-bearing horizons. The Um Tina and Abu Ruweis formations are bedded, fine grained clastic deposits, usually deposited in more or less saline conditions, and deviate most from the Keuper, which contains many sandy units in the German Basin. However, generally, these southern Tethyan deposits of a shallow sea, possibly wide open to the ocean, are rather similar to the northern deposits of a shallow sea in Central Europe that have quite restricted connections to the Tethys Ocean (Szulc 2000). They can be also seen in southern Israel, in the Mohilla Formation. This may indicate that the accessibility of



Text-fig. 1. Locality maps. A. General location of the studied area (asterisk). B. Geology of the Wadi-Hisban area (after Shawabkeh, 2001).

the open ocean to this Near East Triassic basin was also not as open as thought, and there were lands to the north that separated the basin from the ocean.

Between the Late Permian and the Late Triassic, Gondwana continued to drift northward as an integral part of Pangea. According to Schandelmeier *et al.* (1997), Jordan has moved from latitude 20°S in the Late Permian across the equator to about 8°N in the Late Triassic. Accordingly, Jordan was located near the equator during the deposition of the limestones of the Hisban Formation, which were deposited in a sedimentary basin located across the Eastern Mediterranean region from NW Egypt to SE Turkey (Text-fig. 1A). The basin was developed in the Late Triassic and Early Jurassic as the result of the breaking-up of the Gondwana palaeocontinent, which caused the separation of the Apulia block from the Afro-Arabian Plate (Dercourt *et al.* 1986; May 1990). During the Triassic, the eastern part of the Apulia block diverged from Arabia, causing a regional extension, leading to the formation of a failed rift or aulacogen (McBride *et al.* 1990), and the development of a basin in the northern part of Jordan and adjacent parts of Syria (Bandel and Khoury 1981;

Shinaq 1996). The rifting was initiated in the Middle Anisian (May 1990; Shinaq 1996). This basin is considered to be an embayment of the Neotethys (May 1990), the axis of which in the Middle Triassic had an orientation NW-SE, and sediments generally become thinner to the SE (Shinaq 1996).

The Hisban Formation and the studied section

The Hisban Formation belongs to the Ramtha Group, which encompasses all the Triassic deposits of Jordan (Shinaq 1996). This formation is lithostratigraphically equivalent to the Ra'af Formation that is exposed in the Negev of Israel (Weissbrod 1969; Bandel and Khoury 1981; Bandel and Waksmundzki 1985), the lower part of the Geli Khana Formation in northern Iraq, and the Kurra Chine Formation in Syria and Iraq (see Shinaq 1996).

The name of the Hisban Formation (Abu Hamad 2004) derives from Wadi Hisban (Text-fig. 1A, B), where outcrops of the Triassic rocks were found and described in an unpublished report by Wetzel (1947). It was known as the Hisban Limestone (Wetzel and Morton 1959), the Lower Wadi Hisban Sandstone, "Muschelkalk" and Sandy Marl (Bender 1968), and the Hisban Limestone Formation (Basha 1981). The Hisban Formation is exposed along the northeastern shore of the Dead Sea from Wadi Nakhla in the south to Wadi Hisban in the north (NE corner of the Dead Sea) and then further north in Wadi Abu Oneiz (12 km west of the town of Naur, Text-fig. 1). It has also been encountered in wells in the NW and NE of Jordan. Makhlof (1998) reported that the section of this formation in Wadi Hisban, with an average thickness of 30 m, is incomplete. Therefore, he proposed a new type section in Wadi Nakhla, which is 35 m thick. However, Sadeddin (1998), Shawabekeh (1998) and NSJC (2000) still considered the Wadi Hisban section as the type section of their "Hisban Limestone Formation". In Wadi Dardur, the Hisban Formation is 35 m thick (Bandel and Khoury 1981) as confirmed by Andrews *et al.* (1992), Makhlof *et al.* (1996), Shawabekeh (1998), Makhlof (1999) and NCJSC (2000).

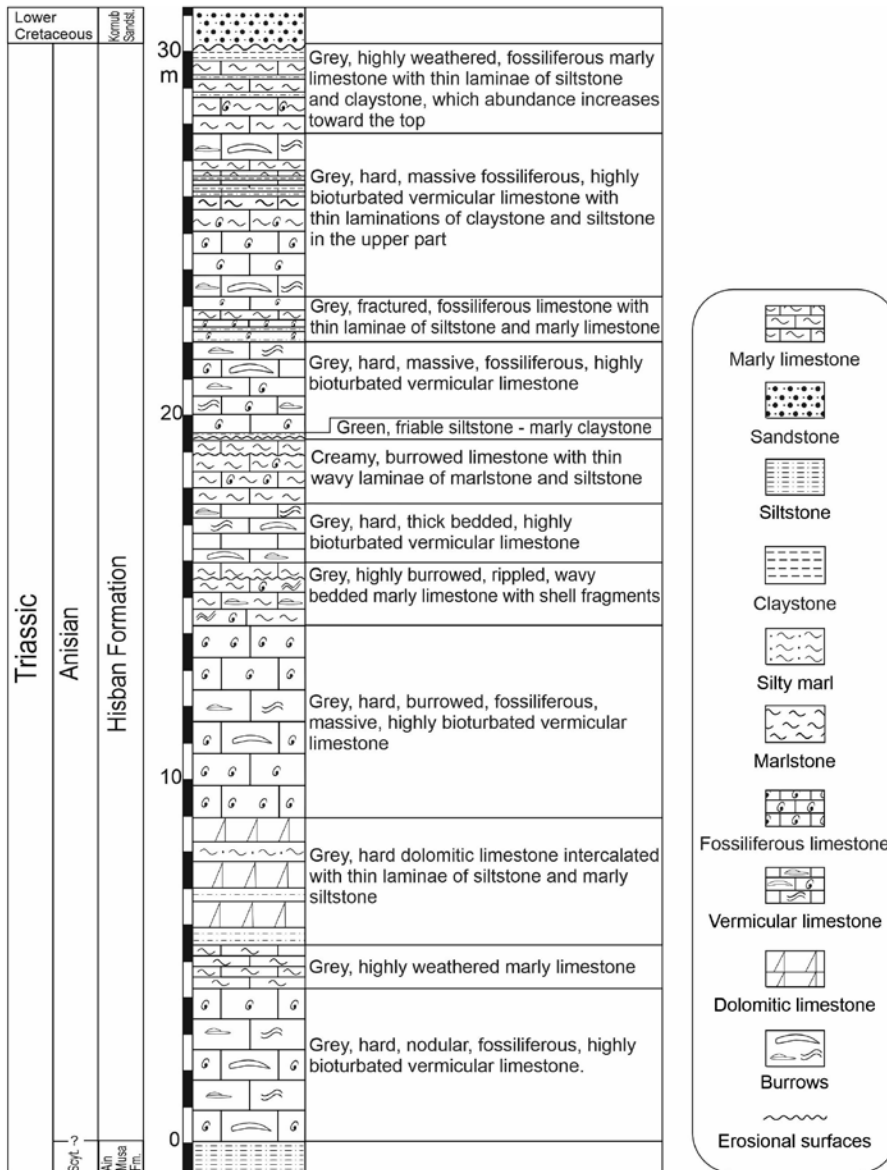
In Wadi Hisban, the base of the Hisban Formation is not exposed, and the top is truncated by an unconformity at the base of the Cretaceous deposits. About 20 km south in the Wadi Nakhla, a complete section is well exposed, which conformably overlies the Ain Musa Formation and underlies the Mukheiris Formation. The base and top of the Hisban Formation can also be seen in Wadi Mukheiris and Wadi Dardur, where the base is marked by a sharp contact between

the green-grey marlstone-siltstone of the Ain Musa Formation and the massive limestone of the basal unit of the Hisban Formation. Limestone-to-marl and sandy marl intercalations at the top of the Hisban Formation transit rapidly into the cross-bedded sandstones at the base of the Mukheiris Formation. This boundary is well exposed in Wadi Mukheiris.

The Hisban Formation represents a "pre-rift" stage of the basin development (Shinaq 1996). As exposed in Wadi Hisban and Wadi Dardur, it is considered to be shallow marine, but located relatively far from shore (Bandel and Khoury 1981). This has also been suggested by Sadeddin (1998) and Shawabekeh (1998) and similar conditions were reported from wells drilled in northern Jordan (e.g., the NH-2 well). Makhlof (1999) suggested subtidal conditions for the lower part of the formation, which changed to intertidal up the section.

Primarily, the Hisban Formation has been dated to the middle Late Triassic on the basis of bivalves, gastropods, and ammonites (Cox 1924, 1932; Wagner 1934). Wetzel and Morton (1959) suggested an Anisian to early Ladinian age, and Parnes (1975) an early Anisian age. Based on conodonts and holothurian sclerites, Sadeddin (1992, 1998) assigned an early-late Anisian age. The Hisban Formation as exposed in Wadi Abu Oneiz was assigned to the middle Anisian (Pelsonian), based on conodonts (Abu Hamad 1994). Based on palynomorphs, Abu Hamad (2004) and Bandel and Abu Hamad (2013) related the Hisban Formation to the palynomorph *Aratrisporites saturnii* Zone of the late Anisian (late Pelsonian-Illyrian).

In the present study, a 30 m-thick section of the Hisban Formation in Wadi Hisban is presented, where it forms limestone cliffs (Text-figs 2, 3). The location of the studied section is shown on the geological map of the study area (Text-fig. 4). In the lower part of the section, grey, wavy-bedded dolomitic limestone beds, up to 20 cm thick, are present. The section consists predominantly of vermicular limestones (their name comes from well-visible and dense bioturbation structures; cf. Bandel and Khoury 1981). The vermicular limestones are composed of medium- to very thick bedded, grey to light brown, nodular, fossiliferous, stylolitic mudstones/wackstones and yellowish marly calcisiltites with wavy bedding. They are commonly highly porous. Marly calcisiltites contain quartz grains and iron (hydro-) oxides. The rocks are yellowish to reddish weathered. The vermicular limestones are interbedded with thin intercalations of siltstones, marlstones, and very thinly laminated mudstones, marked in the morphology of the cliffs by gentle slope escarpments. They contain fossils of



Text-fig. 2. Lithostratigraphic log of the studied section (based on the field work in 2020). Scyt. – Scythian.

bivalves, including oysters, as well as brachiopods and crinoids.

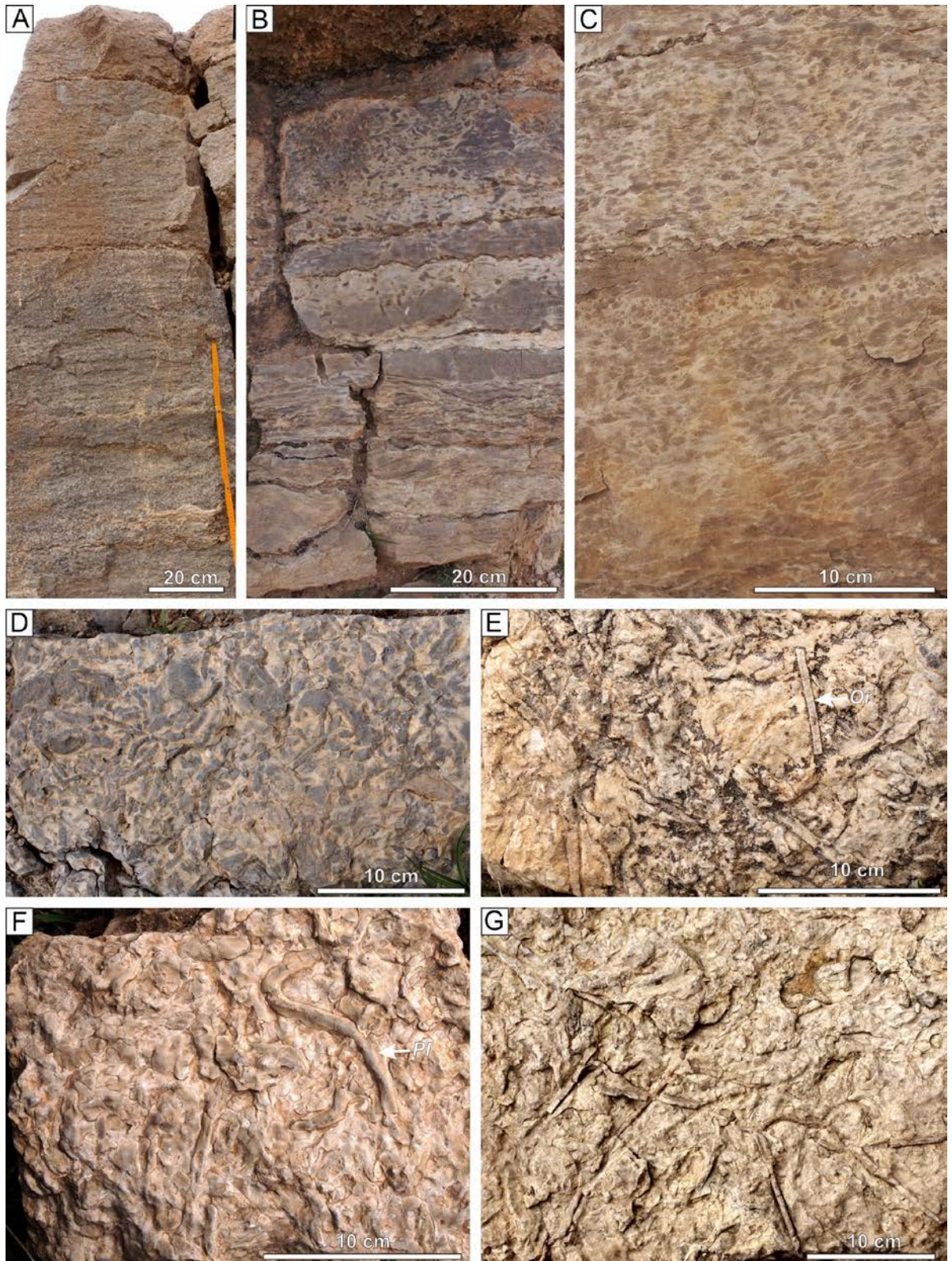
TRACE FOSSILS AND ICHNOFABRICS

The trace fossils and ichnofabrics from the vermicular limestones were studied in the field and photographically documented. Several samples were taken for more detailed studies in the laboratory, and some of these are housed in the Institute of Geological Sciences of the Jagiellonian University in Kraków.

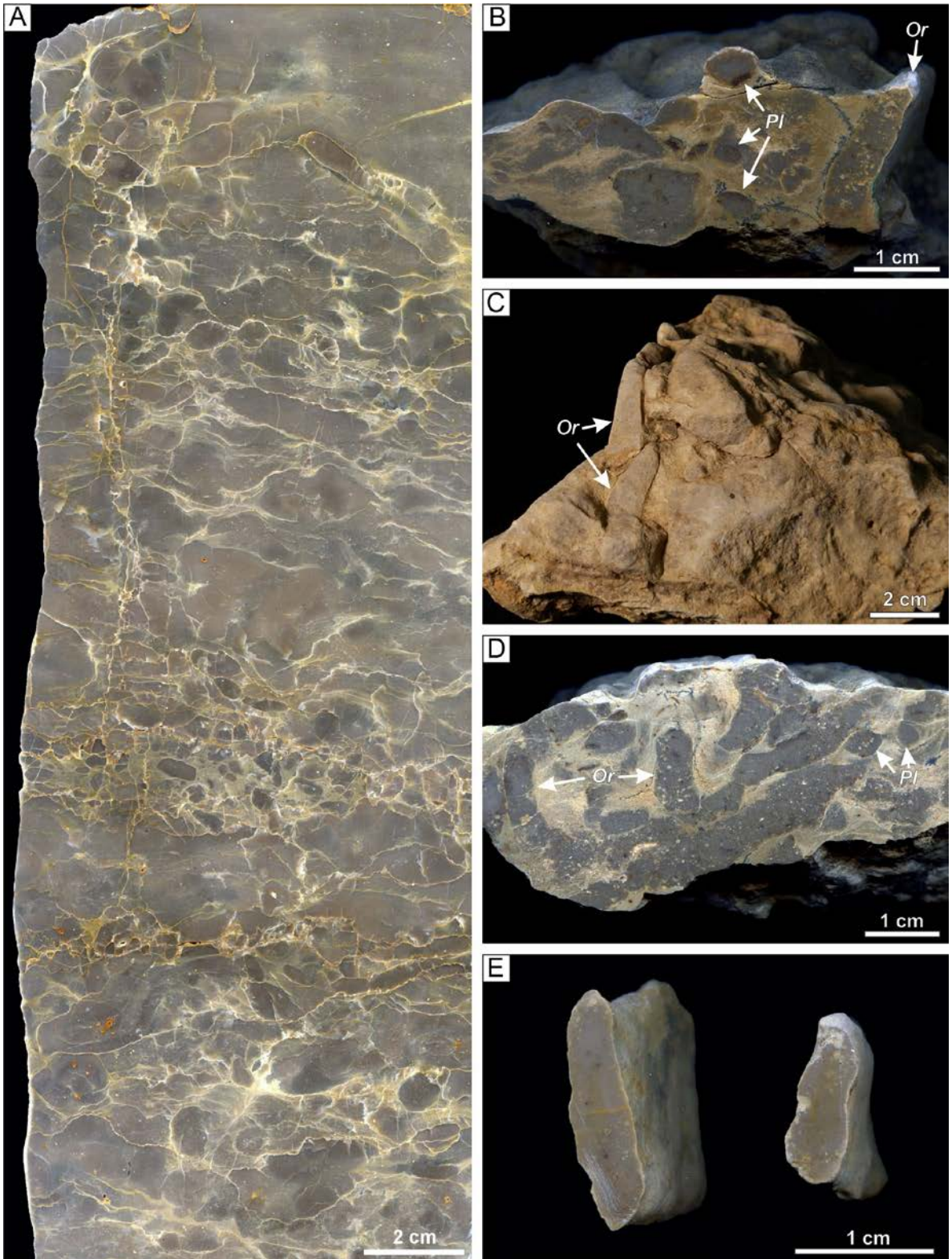
Description of trace fossils

Oravaichnium carinatum Stachacz, Knaust and Matysik, 2022
(Text-figs 3E, G, 4B–E)

DESCRIPTION: Hypichnial, straight, curved or slightly winding horizontal, slightly oblique or arcuate, wall-like ridges, 3–6 mm wide, 3–20 mm high, or endichnial burrows with an irregular, angular, carinate or wedge-shaped cross section. The shape and width vary in individual burrows, but most specimens



Text-fig. 3. Field photos of the vermicular limestone of the Hisban Formation. A–C. Weathered vertical walls showing dense *Planolites*–*Oravaichnium* ichnofabric. D–G. Bedding plane view of bioturbated limestone beds on the upper; *Or* – *Oravaichnium carinatum*, *Pl* – *Planolites beverleyensis*.



Text-fig. 4. *Oravaichnium* and *Planolites* from the Hisban Formation. A. Polished vertical slab showing *Planolites*–*Oravaichnium* ichnofabric. B. *Oravaichnium carinatum* (*Or*) and *Planolites beverleyensis* in a bioturbated limestone bed. C. *Oravaichnium carinatum* (arrowed), lower bedding plane. D. *Oravaichnium carinatum* – transitional form to *O. hrabei* (*Or*) and *Planolites beverleyensis* (*Pl*) in a bioturbated limestone bed; faecal pellets (light, circular to oval spots) are visible. E. Cross sections of *Oravaichnium carinatum* extracted from marly matrix.

show wedge-shaped, downward tapering cross-sections. The fill of the burrow is massive, occasionally with scattered, ellipsoidal faecal pellets cf. *Coprulus oblongus* Mayer, 1952. The pellets are micritic, lighter in colour than the burrow fill, ca. 0.3 mm in diameter and ca. 0.5 mm long (Text-fig. 4B, D, E).

REMARKS: *Oravaichnium carinatum* is the main component of the ichnoassemblage in the Hisban Formation. Some specimens resemble *Planolites beverleyensis* (Billings, 1862), but the latter differs by its having a circular or semi-circular cross-section. *Oravaichnium* is interpreted as a bivalve trace fossil (Uchman *et al.* 2011). *Oravaichnium carinatum* differs from *O. hrabei* Plička and Uhrová, 1990, by having a carinate instead of a sub-rectangular cross-section (Stachacz *et al.* 2022; see also Uchman *et al.* 2011). The precise distinction between them requires measuring the width of the burrow at 1/3 and 2/3 of its height. The ratio of these parameters for *O. carinatum* from the Germanic Basin is 0.73–0.93, while that for *O. hrabei* is approximately 1 (Stachacz *et al.* 2022). However, transitional forms between these two ichnospecies are present. Among specimens from the Hisban Formation, burrows with a strongly elongated wedge shape with straight and smooth margins dominate, whereas specimens from the Germanic Basin mainly have a pear-shaped cross-section (Stachacz *et al.* 2022). In this stage of recognition, both morphotypes fall under the ichnospecies *O. carinatum*. *Oravaichnium oualimehadjensis* Naimi and Cherif, 2021, has a similar, but more rounded cross-section, a strongly winding course, and a very large termination. According to the diagnosis and illustrations of that ichnospecies, it can be considered a transitional trace from *Oravaichnium* to *Lockeia* (cf. Stachacz *et al.* 2022).

Planolites beverleyensis (Billings, 1862)
(Text-figs 3D, F, 4A, B, D)

DESCRIPTION: Hypichnial, horizontal, straight or curved, smooth ridge, or endichnial cylindrical burrows, circular or elliptical in cross-section. The observed burrows are 5–20 mm wide and at least up to 10 cm long, with massive filling, which is usually darker than the host rock.

REMARKS: Some specimens are similar to *Palaeophycus tubularis* Hall, 1847, because of indistinct colour differences between the infill and host rock. *Planolites beverleyensis* is also similar to poorly preserved *Oravaichnium carinatum*, if it is

observed only on the bedding plane. *Planolites* is a deposit feeding structure produced by variable organisms (e.g., Pemberton and Frey 1982; Fillion and Pickerill 1990).

Palaeophycus tubularis Hall, 1847
(Text-fig. 5A, B)

DESCRIPTION: Hypichnial, straight, occasionally branched convex ridge or endichnial cylindrical burrows, 5–10 mm wide and up to at least 200 mm long, circular to oval in cross section. It has a distinct to indistinct, smooth wall and is filled with the same material as the host rock.

REMARKS: The illustrated specimens partly have a relatively thick wall and resemble *Palaeophycus heberti* (Text-fig. 5B, right). Some specimens are difficult to differentiate from small specimens of *Planolites beverleyensis* due to the visibility of the wall. *Palaeophycus* is interpreted as a burrow produced by carnivores or deposit feeding vermiform organisms (e.g., Pemberton and Frey 1982; Fillion and Pickerill 1990).

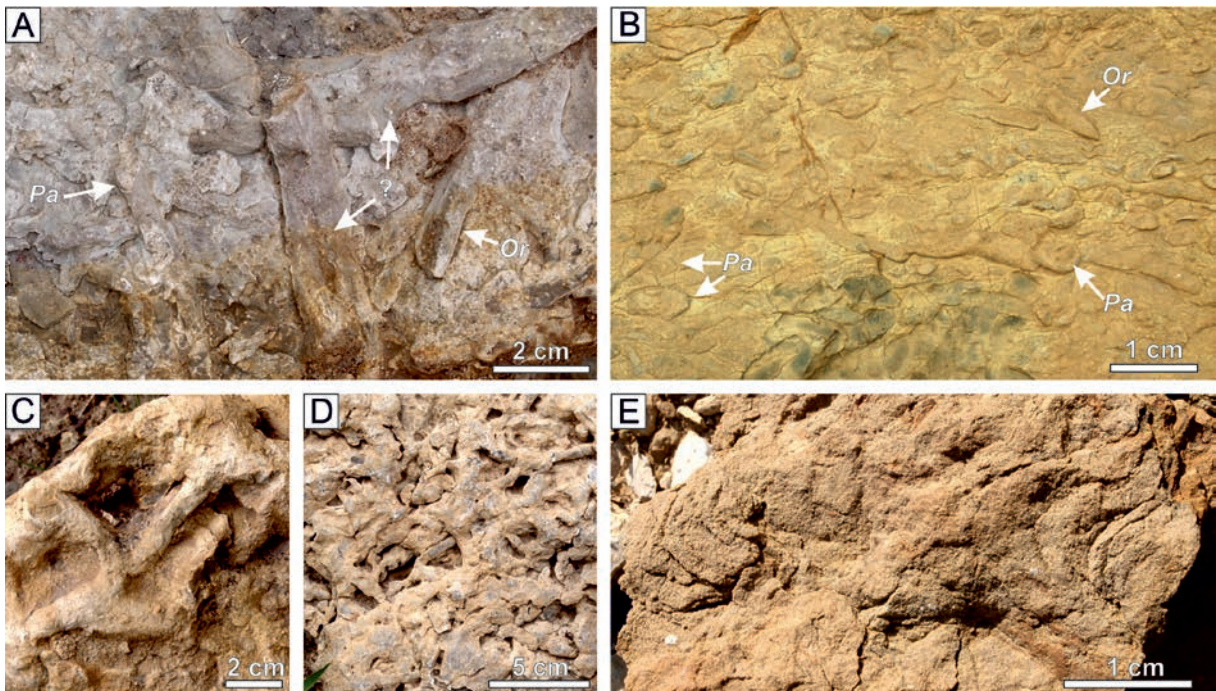
Thalassinoides suevicus (Rieth, 1932)
(Text-fig. 5C, D)

DESCRIPTION: A three-dimensional complex burrow system composed of horizontal, Y-shaped branched tunnels. The burrow tunnels are circular or irregular in cross section and filled with the same substrate as the host deposit. The width of the tunnels is approximately 8–10 mm.

REMARKS: *Thalassinoides* is a dwelling and feeding structure produced mainly by decapod crustaceans, foremost in shallow marine deposits (e.g., Fürsich 1973; Frey *et al.* 1978, 1984; Ekdale 1992; Bromley 1996; Schlirf 2000).

Rhizocorallium commune Schmid, 1876
(Text-fig. 5E)

DESCRIPTION: Endichnial, horizontal, essentially U-shaped, rarely irregular burrow with a distinct marginal tube forming limbs and spreite between them. The marginal tube is 15–25 mm wide, the whole structure is 60–80 mm wide and about 100 mm long. Some fragmentarily preserved burrows are represented only by portions of the marginal tubes that are occasionally flattened with lobate surfaces (Text-fig. 5A).



Text-fig. 5. Trace fossils of the Hisban Formation. A, B. *Palaeophycus tubularis* (*Pa*) associated with *Oravaichnium carinatum* (*Or*) and undetermined burrows (?). C, D. *Thalassinoides suevicus*. E. *Rhizocorallium commune*.

REMARKS: The described trace fossil is poorly preserved and occurs in strongly bioturbated beds. The portions are represented by a flat, lobate marginal tube resembling *Curvolithus* isp. *Rhizocorallium* is produced by suspension feeders (only short oblique, retrusive forms) or deposit feeders, mostly crustaceans (Fürsich 1974; Schlirf 2000) or annelids (Knaust 2013), mainly in shallow marine and marginal marine deposits (e.g., Farrow 1966; Hakes 1976; Knaust 2013).

Ichnofabrics

The vermicular limestones of the Hisban Formation show 2–6 cm-thick intervals of deposits bioturbated in 10–60% (ichnofabric index $ii = 3-4$, according to the scale of Droser and Bottjer 1986; see also Knaust 2012, 2021), alternating with deposits bioturbated in 60–100% ($ii = 5-6$). Rarely, unbioturbated, isolated layers, up to 2 cm thick, are visible. They show many types of undulated or horizontal, irregular burrow fillings, which form the characteristic vermiform pattern. Most of the burrows belong to *Oravaichnium carinatum*, with a changing but always subordinate contribution of *Planolites* (see Text-figs 3D–G, 4A). This is a feature of the *Oravaichnium* ichnofabric sensu Stachacz and Matysik (2020), which is mostly

visible in vertical sections of polished slabs and weathered surfaces as irregular, sub-rectangular or wedge-shaped polygons, or sub-cylindrical spots. In bedding plane views, it is visible mostly as horizontal ridges. Moreover, the relatively uncommon trace fossils *Planolites beverleyensis* and *Palaeophycus tubularis*, plus rarely flattened *Rhizocorallium commune* occur (Text-figs 3–5). Variable proportions of *Planolites/Oravaichnium* in the bioturbated packages can also be observed, but in most cases, the bivalve burrow *Oravaichnium* predominates.

DISCUSSION

The Middle Triassic vermicular limestones occur widespread in the Western Tethys region, both on its northern and southern margins (Text-fig. 6). Baud (1976) described the Triassic trace fossils from the vermicular limestones of the Briançonnais Zone in the Western Alps, and mentioned occurrences of this type of facies in Turkey, Iran and Pakistan. Similar bioturbated limestones were also recognized in the Northern Calcareous Alps (Rüffer and Bechstädt 1998) and the Southern Alps (Maurer and Schlager 2003). Kotański (1986) reported similar fa-



Text-fig. 6. Occurrences of the vermicular limestones (simplified palaeogeographical map for the Ladinian, after Scotese 2013; NW Peri-Tethys range during the Anisian after Szulc 2000). 1: Jordan, this study, 2: Tatricum Basin, Tatra Mts., Poland (Jaglarz and Uchman 2010), 3: Catalan Basin, Betic Cordillera, S Spain (Kotański 1986; Mercedes-Martín and Buatois 2021), 4: Sephardic Domain, Corsica-Sardinia Block, Sardinia, Italy (Knaust and Costamagna 2012), 5: Germanic Basin, Silesia, Poland (Stachacz and Matysik 2020; Stachacz *et al.* 2022), 6: Germanic Basin, Thuringia, Germany (Stachacz *et al.* 2022), 7: Germanic Basin, France (Stachacz *et al.* 2022), 8: Dolomites, S Alps, Italy (Baud 1976; Maurer and Schlager 2003), 9: WN Calcareous Alps, E Alps, Austria (Rüffer and Bechstädt 1998), Middle Prealps, W Alps, W Switzerland and Chablais, France (Baud 1976), 10: Turkey (Baud, 1976), 11: Moro Mts., Iran (Abbassi *et al.* 2015), 12: Pakistan (Baud 1976), 13: Rif Mts., N Morocco (Kotański 1986), 14: Sicily, Italy (Kotański 1986), 15: Calabria, S Italy (Kotański 1986), 16: Greater Kabylia, Algeria (Kotański *et al.* 2004), 17: Levant Basin, Israel (Korngreen and Bialik 2015), 18: Silicium Domain, W Carpathians, N Hungary (Hips 1998), Mecsek and Villány Mts., W Carpathians, S Hungary (Török 1998), 19: Tatricum Domain, Malé Karpaty, W Carpathians, Slovakia (Michalik *et al.* 1992; Šimo 2005).

cies from southern Spain (see also Mercedes-Martín and Buatois 2021), Morocco, Sicily and Calabria, southern Italy, and Kotański *et al.* (2004) mentioned Anisian vermicular limestones from Algeria. Similar facies were also recognized in the Anisian succession from south Israel (Korngreen and Bialik 2015). Lower and Middle Triassic bioturbated limestones were described from the Hungarian Carpathians (Hips 1998; Török 1998). Such limestones were described in detail from the Middle Triassic succession in the Carpathians, in the Polish part of the Tatra Mts. (Jaglarz and Uchman 2010; Rychliński and Uchman 2010) and the Malé Karpaty (Šimo 2005). Strongly bioturbated calcilutites of the Muschelkalk in the Germanic Basin in Upper Silesia, Poland, also contain vermicular limestones (Stachacz and Matysik 2020; Stachacz *et al.* 2022). So far, the discussed vermicular limestones in Jordan are the southeastern-most occurrence of this facies. The *Oravaichnium* ichnofabric was recognized here, in which *Oravaichnium*

prevails and co-occurs with *Planolites*, sometimes it being difficult to distinguish between them.

This mass development of small burrowing bivalves, possibly nuculids, occurred here during the prolonged recovery of benthic populations after the Permian–Triassic mass extinction and was preceded by the rapid development of polychaetes, responsible for the formation of the *Rhizocorallium* ichnofabric (Stachacz and Matysik 2020). A similar record of benthic development during the Triassic recovery, but slightly diachronically and usually with poorly recognized bivalve bioturbation, is observed in many places worldwide (e.g., Chen and Benton 2012; Luo *et al.* 2017; Feng *et al.* 2017, 2018).

Thick packages of the vermicular limestones of the Hisban Formation show the *Oravaichnium* ichnofabric. This suggests that foremost small bivalves and [to] lesser degree vermiform organisms, presumably polychaetes, bioturbated the sediment effectively during ca. 2 ma (approximate length of the late

Pelsonian–Illyrian). The less bioturbated horizons represent rapidly deposited event beds, probably tempestites (Text-fig. 2A, C), which the burrowing benthos did not have time to bioturbate. The low abundance of *Rhizocorallium* is puzzling, considering that this ichnotaxon occurs abundantly in the Middle Triassic rocks worldwide (e.g., Knaust 2013). According to Stachacz and Matysik (2020) and Stachacz (2023), the significant development of the bivalves forming *Oravaichnium* occurred after an earlier explosion of polychaetes producing *Rhizocorallium*. Nevertheless, according to these authors, both of these ichnogenera coexisted in many sections of the Germanic Basin. The scarcity of *Rhizocorallium* is also a feature of the Anisian vermicular limestone of the Tatra Mountains in Poland, where hypersaline conditions are recognized (Jaglarz and Uchman 2010; Rychliński and Uchman 2010). Stachacz (2023) noted that *Rhizocorallium* in the Muschelkalk-Keuper transition in Upper Silesia, Poland, appeared when the salinity potentially increased from oligohaline to polyhaline conditions (see Pawlak *et al.* 2022) and rapid, significant changes in salinity took place during bioturbation. It is not excluded that the environment of the Hisban Formation was also influenced by increased salinity.

The absence or rarity of large *Rhizocorallium* may also mean that the Hisban Formation population has not yet recovered since the end-Permian–Triassic extinction level (stage 4 of Twitchett 2006) (Feng *et al.* 2017, 2018). Otherwise, this may be the result of a slightly deeper environment (cf. Knaust 2013). A different situation was observed by Stachacz and Matysik (2020) in the Polish Muschelkalk, where the presence of large and abundant *Rhizocorallium* is interpreted as the penultimate stage of recovery (before the middle to late Pelsonian), and generally occurred before the great bivalve infaunalization and *Oravaichnium* ichnofabric formation. The Triassic of Sardinia, which contains numerous bivalve burrows as well as *Rhizocorallium* (Knaust and Costamagna 2012), shows a slightly later recovery that took place in the Anisian.

The ichnological record in the Hisban Formation exhibits particularly close similarities to the Triassic of the Germanic Basin from the territory of Poland and Germany, i.e., in the other, northern Peri-Tethys. This shows that burrows of bivalves are much more common and widespread in the Middle Triassic than previously thought. The small bivalves, most likely nuculids, played a significant role in bioturbation and infaunalization of the Middle Triassic, and it should be recognized as one of the most important stages of the Triassic ichnocoenosis evolution. Further studies of the Triassic vermicular limestones may test this idea.

CONCLUSIONS

The Anisian Hisban Formation in Jordan (southern Peri-Tethys) is formed of a moderately to strongly bioturbated (10–100% of bioturbated deposit) vermicular limestone facies, which shows the monotonous *Oravaichnium*–*Planolites* ichnofabric.

Oravaichnium carinatum is the most common trace fossil in the formation, and it is responsible for strong bioturbation, as is similarly the case in some areas of the northern Peri-Tethys and the Germanic Basin, with only small morphological differences.

Oravaichnium carinatum from the Hisban Formation is typically smooth and strongly elongated in the vertical axis, whereas specimens from the Germanic Basin mainly have a pear-shaped cross-section. Nevertheless, transitional morphotypes between them are present in both areas.

The dominance of the *Oravaichnium* ichnofabric in the northern and southern Peri-Tethys suggests that small burrowing bivalves played a significant role in the long-term recovery of the benthos after the Permian–Triassic crisis and were responsible for the infaunalization and its extensive bioturbation during the Middle Triassic.

Acknowledgements

The research of M.S. and A.U. was supported by the Strategic Programme Excellence Initiative from the Jagiellonian University. The field work of AU in Jordan was enabled by the Erasmus+ programme and was supported by the University of Jordan. An anonymous reviewer is acknowledged for valuable remarks and constructive comments.

REFERENCES

- Abbassi, N., Shabanian, R. and Hamede Golparvar, R. 2015. Environmental impacts on the ichnofossil diversity of the lower part of the Elika Formation (Lower Triassic), Moro Mountain, NW Iran. *Iranian Journal of Science & Technology*, **39A3**, 273–280.
- Abu Hamad, A. 1994. Stratigraphy and Microfacies of The Triassic in Wadi Abu Oneiz Area (West Na'ur). Unpublished M.Sc. Thesis, 107 pp. Yarmouk University; Irbid.
- Abu Hamad, A. 2004. Paläobotanik und Palynostratigraphie der Permo-Trias Jordaniens: Palaeobotany and Palynostratigraphy of the Permo-Triassic in Jordan. Unpublished Ph.D. Thesis, 316 pp. University of Hamburg; Hamburg.
- Andrews, I., Makhlof, I., Taani, Y., Al-Bashish and Al-Hiari, A. 1992. Permian, Triassic and Jurassic lithostratigra-

- phy in the subsurface of Jordan. *Subsurface Geology Division Bulletin*, **4**, 98 pp.
- Bandel, K. and Abu Hamad, A. 2013. Permian and Triassic strata of Jordan. In: Tanner, L.H., Spielmann, J.A. and Lucas, S.G. (Eds), *The Triassic System. New Mexico Museum of Natural History and Science, Albuquerque, Bulletin*, **61**, 31–41.
- Bandel, K. and Khoury, A. 1981. Lithostratigraphy of the Triassic in Jordan. *Facies*, **4**, 1–26.
- Bandel, K. and Waksmundzki, B. 1985. Triassic conodonts from Jordan. *Acta Geologica Polonica*, **35**, 239–304.
- Basha, S.H. 1981. Distribution of Triassic rocks in Jordan and Levant. *Dirasat*, **8**, 49–67.
- Baud, A. 1976. Les terriers de Crustacés décapodes et l'origine de certains faciès du Trias carbonaté. *Eclogae Geologicae Helvetiae*, **69**, 415–424.
- Bender, F. 1968. Geologie von Jordanien. Beiträge zur regionalen Geologie der Erde, 230 pp. Borntraeger Verlag; Stuttgart-Berlin.
- Billings, E. 1862. New species of fossils from different parts of the Lower, Middle and Upper Silurian rocks of Canada. In: *Palaeozoic Fossils, Volume 1 (1862–1865)*, 96–168. Geological Survey of Canada, Dawson Brothers; Montreal.
- Bromley, R.G. 1996. Trace Fossils, Biology, Taphonomy and Applications, Second edition, 361 pp. Chapman & Hall; London.
- Chen, Z.Q. and Benton, M.J. 2012. The timing and pattern of biotic recovery following the end-Permian mass extinction. *Nature Geoscience*, **5**, 375–383.
- Cox, L.R. 1924. Triassic fauna from the Jordan Valley. *Annals and Magazine of Natural History*, **14**, 52–96.
- Cox, L.R. 1932. Further notes on the Trans-Jordan Trias. *Annals and Magazine of Natural History*, **10**, 93–113.
- Dercourt, J., Zonenshain, C.P., Ricou, L.-E., Kazmin, V.G., Le Pichon, X., Knipper, A.L., Grandjacquet, C., Sbotshikov, I.M., Geysant, J., Lepvrier, C., Pechersky, D.H., Boulin, J., Sibuet, J.-C., Savostin, L.A., Sorokhtin, O., Westphal, M., Bazhenov, M.I., Lauer, J.P. and Biju-Duval, B. 1986. Geological evolution of the Tethys belt from the Atlantic to the Pamirs since the Lias. *Tectonophysics*, **123**, 241–315.
- Droser M.L. and Bottjer D.J. 1986. A semiquantitative field classification of ichnofabric. *Journal of Sedimentary Petrology*, **56**, 558–559.
- Ekdale, A.A. 1992. Muckraking and mudslinging: the joys of deposit feeding. In: Maples, C.G. and West, R.R. (Eds), *Trace Fossils*, 145–171. Paleontological Society Short Course 5; Cambridge.
- Farrow, G.E. 1966. Bathymetric zonation of Jurassic trace fossils from the coast of Yorkshire, England. Bathymetric zonation of Jurassic trace fossils from the coast of Yorkshire, England. *Palaeogeography, Palaeoclimatology, Palaeoecology*, **2**, 103–151.
- Feng, X., Chen, Z.-Q., Woods, A., Pei, Y., Wu, S., Fang, Y., Luo, M. and Xu, Y. 2017. Anisian (Middle Triassic) marine ichnocoenoses from the eastern and western margins of the Kamdian Continent, Yunnan Province, SW China: Implications for the Triassic biotic recovery. *Global and Planetary Change*, **157**, 194–213.
- Feng, X., Chen, Z., Bottjer, D.J., Fraiser, M.L., Xu, Y. and Luo, M. 2018. Additional records of ichnogenus *Rhizocorallium* from the Lower and Middle Triassic, South China: Implications for biotic recovery after the end-Permian mass extinction. *Geological Society of America Bulletin*, **130**, 1197–1215.
- Fillion, D. and Pickerill, R.K. 1990. Ichnology of the Upper Cambrian? to Lower Ordovician Bell Island and Wabana groups of eastern Newfoundland, Canada. *Palaeontographica Canadiana*, **7**, 1–119.
- Frey, R.W., Howard, J.D., Bromley, R.G. and Pryor, W.A. 1978. *Ophiomorpha*: its morphologic, taxonomic and environmental significance. *Palaeogeography, Palaeoclimatology, Palaeoecology*, **23**, 199–229.
- Frey, R.W. Curran, A.H. and Pemberton, S.G. 1984. Tracemaking activities of crabs and their environmental significance: the ichnogenus *Psilonichnus*. *Journal of Paleontology*, **58**, 511–528.
- Fürsich, F.T. 1973. *Thalassinoides* and the origin of nodular limestone in the Corallian Beds (Upper Jurassic) of Southern England. *Neues Jahrbuch für Geologie und Paläontologie*, **2**, 136–156.
- Fürsich, F.T. 1974. Ichnogenus *Rhizocorallium*. *Paläontologische Zeitschrift*, **48**, 16–28.
- Hakes, W.G. 1976. Trace fossils and depositional environment of four clastic units, Upper Pennsylvanian megacyclothem, northeast Kansas. *The University of Kansas, Paleontological Contributions*, **63**, 1–46.
- Hall, J. 1847. *Palaeontology of New York I*, Geological Survey of New York, Albany, C. Van Benthuysen, 338 pp.
- Hips, K. 1998. Lower Triassic storm-dominated ramp sequence in northern Hungary: an example of evolution from homoclinal through distally steepened ramp to Middle Triassic flat-topped platform. In: Wright, V.P. and Burchette, T.P. (Eds), *Carbonate ramps. Geological Society London Special Publication*, **149**, 315–338.
- Jaglarz, P. and Uchman, A. 2010. A hypersaline ichnoassemblage from the Middle Triassic carbonate ramp of the Tatricum domain in the Tatra Mountains, Southern Poland. *Palaeogeography, Palaeoclimatology, Palaeoecology*, **292**, 71–81.
- Knaust, D. 2012. Methodology and techniques. In: Knaust, D. and Bromley, R.G. (Eds), *Trace Fossils as Indicators of Sedimentary Environments. Development in Sedimentology*, **64**, 245–271.
- Knaust, D. 2013. The ichnogenus *Rhizocorallium*: Classification, trace makers, palaeoenvironments and evolution. *Earth-Science Reviews*, **126**, 1–47.
- Knaust, D. 2021. Ichnofabric. In: Elias, S.A. and Alderton, D.

- (Eds), *Encyclopedia of Geology* (Second Edition), 520–531. Academic Press; London.
- Knaust, D. and Costamagna, L.G. 2012. Ichnology and sedimentology of the Triassic carbonates of north-west Sardinia, Italy. *Sedimentology*, **59**, 1190–1207.
- Korngreen, D. and Bialik, O.M. 2015. The characteristics of carbonate system recovery during a relatively dry event in a mixed carbonate/siliciclastic environment in the Pelsonian (Middle Triassic) proximal marginal marine basins: A case study from the tropical Tethyan northwest Gondwana margins. *Palaeogeography, Palaeoclimatology, Palaeoecology*, **440**, 793–812.
- Kotański, Z. 1986. Faciès alpins triasiques dans la Méditerranée occidentale. *Przegląd Geologiczny*, **34**, 627–635. [In Polish with French summary]
- Kotański, Z., Gierliński, G. and Ptaszyński, T. 2004. Reptile tracks (*Rotodactylus*) from the Middle Triassic of the Djurdjura Mountains in Algeria. *Geological Quarterly*, **48**, 89–96.
- Luo, M., Shi, G. R., Hu, S., Benton, M.J., Zhong-Qiang, C., Jinyuan, H., Qiyue, Z., Changyong, Z. and Wen, W. 2017. Early Middle Triassic trace fossils from the Luoping Biota, southwestern China: evidence of recovery from mass extinction. *Palaeogeography, Palaeoclimatology, Palaeoecology*, **515**, 6–22.
- Makhlouf, I.M. 1998. Facies analysis of the Triassic Ain Musa Formation, Dead Sea, Jordan. *Abhath Al-Yarmouk*, **8**, 93–110.
- Makhlouf, I.M. 1999. Shallowing-upward facies of the Triassic Hisban Limestone Formation in Jordan. *Journal of Al-Manarah*, **4**, 259–274.
- Makhlouf, I.M., Al-Hiyari, A., Al-Bashish, M. and Abu Azzam, H. 1996. Sedimentological and lithostratigraphy of the Triassic strata of Jordan at outcrop and in the subsurface. *Subsurface Geology Bulletin*, **7**, 1–79. Geology Directorate, National Resources Authority, Amman.
- Maurer, F. and Schlager, W. 2003. Lateral variation in sediment composition and bedding in Middle Triassic interplatform basins (Buchenstein Formation, Southern Alps, Italy). *Sedimentology*, **50**, 1–22.
- May, P.R. 1990. The eastern Mediterranean Mesozoic basin: evolution and oil habitat. *American Association of Petroleum Geologists Bulletin*, **75**, 1215–1232.
- Mayer, G. 1952. Neue Lebensspuren aus dem Unteren Hauptmuschelkalk (Trochitenkalk) von Wiesloch: *Coprulus oblongus* n. sp. und *C. sphaeroideus* n. sp. *Neues Jahrbuch für Geologie und Paläontologie, Monatshefte*, **1952**, 376–379.
- McBride, J.J., Barazangi, M., Best, J., Al-Saad, D., Sawaf, T., Al-Otri, M. and Gebran, A. 1990. Seismic reflection structure of intracratonic Palmyride fold-thrust belt and surrounding Arabian Platform, Syria. *American Association of Petroleum Geologists Bulletin*, **74**, 238–259.
- Mercedes-Martín, R. and Buatois, L.A. 2021. Microbialites and trace fossils from a Middle Triassic restricted carbonate ramp in the Catalan Basin, Spain: evaluating environmental and evolutionary controls in an epicontinental setting. *Lethaia*, **54**, 4–25.
- Michalík, J., Masaryk, P., Lintnerová, O., Papšová, J., Jendrejčková, O. and Reháková, D. 1992. Sedimentology and facies of a storm-dominated Middle Triassic carbonate ramp (Vysoká Formation, Malé Karpaty Mts., Western Carpathians). *Geologica Carpathica*, **43**, 213–230.
- Naimi, N.M. and Cherif, A. 2021. *Oravaichnium oualimehadjensis*, a new possible bivalve repichnion from the Upper Jurassic Argiles de Saïda Formation (middle Oxfordian Saïda Mounts, NW Algeria). *Neues Jahrbuch für Geologie und Paläontologie*, **302**, 209–220.
- NCJSC (Nomenclature Committee for the Jordanian Stratigraphic Column), 2000. Internal Report. Part 2, 46 pp. National Resources Authority; Amman.
- Parnes, A. 1975. Middle Triassic ammonite biostratigraphy in Israel. *Geological Survey of Israel Bulletin*, **66**, 1–35.
- Pawlak, W., Rozwalak, P. and Sulej, T. 2022. Triassic fish faunas from Miedary (Upper Silesia, Poland) and their implications for understanding paleosalinity. *Palaeogeography, Palaeoclimatology, Palaeoecology*, **590**, 110860.
- Pemberton, S.G. and Frey, R.W. 1982. Trace fossil nomenclature and the *Planolites*–*Palaeophycus*. *Journal of Paleontology*, **56**, 843–881.
- Plička, M. and Uhrová, J. 1990. New trace fossils from the Outer Carpathians flysch (Czechoslovakia). *Acta Musei Moraviae, Scientiae Naturales*, **75**, 53–59.
- Rieth, A. 1932. Neue Funde spongeliomorpher Fucoiden aus dem Jura Schwabens. *Geologische Paläontologische Abhandlungen, Neue Folge*, **19**, 257–294.
- Rüffer, T. and Bechstadt, T. 1998. Triassic sequence stratigraphy in the western part of the Northern Calcareous Alps (Austria). In: Graciansky, P.C., Hardenbol, J., Jacquin, T. and Vail, P. (Eds), *Mesozoic and Cenozoic sequence stratigraphy of European basins. Society for Sedimentary Geology Special Publication*, **60**, 751–761.
- Rychliński, T. and Uchman, A. 2010. Early and Middle Triassic trace fossils of the Fatricum domain in the Tatra Mountains and their palaeoenvironmental significance. *Przegląd Geologiczny*, **58**, 1079–1086. [In Polish, with English summary]
- Sadeddin, W. 1992. *Acanthotheelia jordanica* n. sp., a new holothurian sclerite species from the Pelsonian (Middle Anisian) of Jordan. *Revista Española de Micropaleontologica*, **23**, 83–88.
- Sadeddin, W. 1998. Conodont – Biostratigraphy and Paleogeography of the Triassic in Jordan. *Palaeontographica Abteilung A, Band A*, **248**, 119–144.
- Schandelmeier, H. and Reynolds, P.-O. 1997. *Palaeogeographic-Palaeotectonic Atlas of North-Eastern Africa, Arabia, and Adjacent Areas*, 160 pp. Balkema; Rotterdam.
- Schlirf, M. 2000. Upper Jurassic trace fossils from the Bou-

- Ionnais (northern France). *Geologica et Palaeontologica*, **34**, 145–213.
- Schmid, E.E. 1876. Der Muschelkalk des östlichen Thüringen, 20 pp. Fromann; Jena.
- Scotese, C.R. 2013. Map Folio 46, Middle Triassic (Landinian, 232.9 Ma), PALEOMAP PaleoAtlas for ArcGIS, volume 3, Triassic and Jurassic Paleogeographic, Paleoclimatic and Plate Tectonic Reconstructions, PALEOMAP Project, Evanston, IL.
- Shawabekeh, K. 1998. The geology of Ma'in area – Map Sheet No. (3155 III) Hashemite Kingdom of Jordan. *Geological Mapping Division Bulletin*, **40**, 1–74. Geology Directorate, National Resources Authority; Amman.
- Shawabekeh, K. 2001. The Geology of Karama Area – Map Sheet No. (3156 III). Hashemite Kingdom of Jordan, *Geological Mapping Division Bulletin*, **48**, 1–79. Geology Directorate, National Resources Authority; Amman.
- Shinaq, R. 1996. Subsurface Triassic sediments in Jordan: stratigraphic and depositional characteristics, and hydrocarbon potential. *Journal of Petroleum Geology*, **19**, 57–76.
- Šimo, V. 2005. Anisian trace fossils from the Vysoká Formation (Slovakia). *Przegląd Geologiczny*, **53**, 884. [In Polish]
- Stachacz, M. 2023. Pioneer colonization, evidenced by *Rhizocorallium* in the Middle Triassic of Poland. *Annales Societatis Geologorum Poloniae*, **93**, 363–379.
- Stachacz, M., Knaust, D. and Matysik, M. 2022. Middle Triassic bivalve traces from central Europe (Muschelkalk, Anisian): overlooked burrows of a common ichnofabric. *PalZ, Paläontologische Zeitschrift*, **96**, 175–196.
- Stachacz, M. and Matysik, M. 2020. Early Middle Triassic (Anisian) trace fossils, ichnofabrics, and substrate types from the southeastern Germanic Basin (Wellenkalk facies) of Upper Silesia, southern Poland: Implications for biotic recovery following the Permian/Triassic mass extinction. *Global and Planetary Change*, **194**, 103290.
- Szulg, J. 2000. Middle Triassic evolution of the northern peri-Tethys area as influenced by early opening of the Tethys Ocean. *Annales Societatis Geologorum Poloniae*, **70**, 1–48.
- Török, Á. 1998. Controls on development of Mid-Triassic ramps: examples from southern Hungary. In: Wright, V.P. and Burchette, T.P. (Eds), Carbonate ramps. *Geological Society London Special Publication*, **149**, 339–367.
- Twitchett, R.J. 2006. The palaeoclimatology, palaeoecology and palaeoenvironmental analysis of mass extinction events. *Palaeogeography, Palaeoclimatology, Palaeoecology*, **232**, 190–213.
- Uchman, A., Mikuláš, R. and Rindsberg, A.K. 2011. Mollusc trace fossils *Ptychoplasma* Fenton and Fenton, 1937 and *Oravaichnium* Plička and Uhrová, 1990: their type material and ichnospecies. *Geobios*, **44**, 387–397.
- Wagner, G. 1934. Deutscher Muschelkalk am Toten Meer. *Natur und Volk*, **64**, 449–454.
- Weissbrod, T. 1969. The subsurface Paleozoic stratigraphy of southern Israel. In: The Paleozoic of Israel and adjacent countries. *Geological Survey of Israel Bulletin*, **47**, 1–23.
- Wetzel, R. 1947. Stratigraphic Sections of Jordan Valley and Dead Sea, 45 pp. Unpublished Report Petroleum Development (Transjordan); Paris.
- Wetzel, R. and Morton, D.M. 1959. Contribution à la Géologie de la Transjordanie. Notes et Mémoires sur le Moyen Orient. In: Dubertret, M.L. (Ed.), *Contributions à la Géologie de la Péninsule Arabique*, **7**, 95–188. Muséum National d'Histoire Naturelle; Paris.

Manuscript submitted: 5th July 2024

Revised version accepted: 10th September 2024